


RESEARCH ARTICLE

White matter and hypoxic hypobaria in humans

Stephen A. McGuire¹  | Meghann C. Ryan² | Paul M. Sherman³ | John H. Sladky³ |
 Laura M. Rowland² | S. Andrea Wijtenburg² | L. Elliot Hong² | Peter V. Kochunov²

¹Department of Neurology, University of Texas Health Science Center, San Antonio, Texas

²Maryland Psychiatric Research Center, Department of Psychiatry, University of Maryland School of Medicine, Baltimore, Maryland

³U.S. Air Force School of Aerospace Medicine, 59MDW-USAFSAM/FHOH, San Antonio, Texas

Correspondence

Stephen A. McGuire, Department of Neurology, University of Texas Health Science Center, 7703 Floyd Curl Drive, San Antonio, TX 78229.

Email: dr.stephen.mcguire@gmail.com

John H. Sladky, 8930 Woodland Pass, Boerne, TX 78006.

Email: john.h.sladky.mil@mail.mil

Funding information

NIH, Grant/Award Numbers: T32MH067533, R01EB015611, U01MH108148, R01MH096263, R01MH094520; U.S. Air Force, Grant/Award Numbers: I-11-44, I-11-10

Abstract

Occupational exposure to hypobaria (low atmospheric pressure) is a risk factor for reduced white matter integrity, increased white matter hyperintensive burden, and decline in cognitive function. We tested the hypothesis that a discrete hypobaric exposure will have a transient impact on cerebral physiology. Cerebral blood flow, fractional anisotropy of water diffusion in cerebral white matter, white matter hyperintensity volume, and concentrations of neurochemicals were measured at baseline and 24 hr and 72 hr postexposure in $N = 64$ healthy aircrew undergoing standard US Air Force altitude chamber training and compared to $N = 60$ controls not exposed to hypobaria. We observed that hypobaric exposure led to a significant rise in white matter cerebral blood flow (CBF) 24 hr postexposure that remained elevated, albeit not significantly, at 72 hr. No significant changes were observed in structural measurements or gray matter CBF. Subjects with higher baseline concentrations of neurochemicals associated with neuroprotection and maintenance of normal white matter physiology (glutathione, *N*-acetylaspartate, glutamate/glutamine) showed proportionally less white matter CBF changes. Our findings suggest that discrete hypobaric exposure may provide a model to study white matter injury associated with occupational hypobaric exposure.

KEYWORDS

diffusion tensor imaging, FLAIR, hypobaric exposure, magnetic resonance spectroscopy, pseudo continuous arterial spin labeling

1 | INTRODUCTION

Occupational exposure to nonhypoxic hypobaria (low atmospheric pressure) is associated with focal (McGuire et al., 2012, 2013, 2014) and diffuse (McGuire et al., 2016) white matter (WM) injury and neurocognitive decline (McGuire et al., 2014). We performed structural and physiological magnetic resonance imaging (MRI) in healthy young air crewmen undergoing hypobaric exposure as part of their routine training and mapped the trajectory of brain changes 24 and 72 hr postexposure. We hypothesized that a single hypoxic/hypobaric exposure would induce transient but detectable changes in cerebral physiology. Our intent was (a) to identify temporal trends in structural and physiological indexes following hypobaric exposure and (b) to investigate the interplay among these parameters. In addition, we postulated that the innate capacity for

neuro-protection and neuro-inflammation might explain individual variances in trends observed postexposure.

Cerebral WM damage due to occupational hypobaric exposure is reported as elevated hyperintensive white matter (WMH) regions volume and count (McGuire et al., 2013; McGuire, Sherman, et al., 2014) observed on T2-weighted fluid-attenuated inversion recovery (FLAIR) images and diffuse reduction in WM integrity as measured by diffusion tensor imaging (DTI) (McGuire et al., 2012). These WM changes can occur in the absence of decompression sickness (DCS) symptoms (McGuire, Sherman, et al., 2014) but may include symptoms observed in mild traumatic brain injury (TBI) including: vertigo, headache, disorientation, slurred speech, incoordination, visual changes, and inappropriate fatigue (Fehily & Fitzgerald, 2017; Hundemer, Jersey, Stuart, Butler, & Pilmanis, 2012; Jersey et al., 2011). These structural changes are also correlated

with a decline in cognitive performance, including attention, processing speed, working memory, and executive functioning (McGuire, Tate, et al., 2014). Such symptoms mirror TBI and other neurological disorders, whereby a rise in WMH burden correlates with reduced axonal integrity (Kochunov et al., 2010, 2011; Tate et al., 2016, 2017) and cognitive abilities (Holleran et al., 2017; Kochunov et al., 2009, 2010; Tate et al., 2017).

Similar pressure-related WM changes have been reported in extreme mountaineers (Fayed, Modrego, & Morales, 2006; Hackett et al., 1998; Zhang et al., 2012) and divers (Connolly & Lee, 2015). The severity of the burden may not correlate with the duration of exposure or the number of exposure episodes (McGuire et al., 2013; McGuire, Sherman, et al., 2014). Additional contributing factors may include physical and mental activity during exposure, elapsed time between exposures, and/or environmental and genetic susceptibility risks (McGuire, Sherman, et al., 2014). The WM changes we reported suggest a radiographic presentation similar to diffuse axonal changes observed in mild TBI (Adams, Graham, Murray, & Scott, 1982; Inglese et al., 2005; Medana & Esiri, 2003; Moen et al., 2014; Skandsen et al., 2010). We posit that these WM changes may be classified as mild TBI due to barotrauma.

We compared structural and functional changes in cerebral WM in subjects exposed to hypobaric versus controls. Using FLAIR, we assessed changes in WMH; using DTI, we noted changes in microstructural integrity. We assessed CBF in both gray matter (GM) and WM using pseudo-continuous arterial spin labeling (pCASL; Alsop et al., 2015). We used proton magnetic resonance spectroscopy ($^1\text{H-MRS}$) to assess concentrations of neurochemicals associated with neuroprotection, inflammation, and function. To estimate the power necessary to measure hypobaric exposure, we studied the physiological variability in structural and physiological indexes of normal volunteers. We previously demonstrated high reproducibility ($N = 3-5$ to detect a 5% change) for structural indexes and intermediate reproducibility ($N = 10-30$ to detect a 5% change) for physiological indexes (McGuire et al., 2017).

2 | METHODS

2.1 | Subjects

Sixty-four male aircrew volunteers (AFC; average age = 21.0 ± 2.7 years, range = 18–33 years) were imaged 24 hr before exposure (baseline) and 24 and 72 hr postexposure. Sixty male controls (NOR; average age = 22.1 ± 4.9 years, range = 18–41 years) underwent a similar protocol at normal atmospheric pressure. All subjects were healthy without hypertension, hyperlipidemia, or diabetes, and fulfilled USAF Flying Class III neurological standards (McGuire, Sherman, et al., 2014). While both male and female subjects were recruited, insufficient female controls prohibited robust analysis, confining primary analysis to male subjects only. Volunteers were recruited from all USAF trainees whose tightly regulated training schedule permitted them to be available for the 2-week study duration without disruption of training; from all volunteers the participants versus controls were randomly selected at time of arrival for the first MRI. No significant age difference was present between exposed subjects and controls ($p = 0.15$). Commencing 7 days prior to the first MRI and continuing throughout the study duration, all subjects

were free of alcohol, drugs/medications, and tobacco. All subjects maintained a consistent meal time, sleep/wake time, and exercise program. Any new or acute illness was disqualifying. Commercial air travel was restricted 7 days prior to the study and continued until completion. Aside from chamber training exposure, all subjects remained at the San Antonio altitude of approximately 660 ft above sea level. To minimize diurnal physiological fluctuations, the 24 and 72 hr MRI scans were administered at the same time as the participant's original baseline scan. To minimize task-related activation, subjects were not subjected to any stimulation during the MRI.

The study was reviewed and approved by the 59th Medical Wing, USAF, Institutional Review Board. Subjects were active duty members of the USAF recruited to serve as exposure subjects or controls for the effects of occupational exposure to extreme hypobaric in aircrew. None had a prior history of exposure to extreme hypobaric occupationally, recreationally, or experimentally. All participants were recruited with strict adherence to the Department of Defense Instruction for Protection of Human Subjects (DoD, 2011). Subject participation was voluntary without commander involvement or knowledge. All subjects provided informed consent prior to participation. Subjects did not receive compensation for participation.

2.2 | Hypobaric exposure procedure

The objective of standard USAF hypobaric altitude chamber training is for early aircrew recognition of hypoxic symptoms while still retaining sufficient cognitive ability to respond (Gentry, Rango, Zhang, & Biedermann, 2017). Standard protocol includes a brief ear and sinus check exposure at 5,000 ft (exposure 12.2 psi/632 mmHg/ambient air O_2 via aviator mask >500 mmHg) followed by 30 min of denitrogenation on 100% O_2 at sea level via an aviator mask. Trainees then ascend to 25,000 ft (exposure 5.45 psi/282 mmHg/ambient air O_2 via aviator mask >200 mmHg) where they remain for 20 min. Trainees remove their aviator masks, redoning with the first onset of hypoxic symptoms. Total duration of mask removal at altitude is approximately 2–4 min with an O_2 saturation reaching 65–75% (exposure 5.45 psi/282 mmHg/ambient air O_2 59 mmHg). Following recovery on 100% O_2 via aviator mask, trainees descend to 18,000 ft for a visual acuity demonstration followed by continued descent to sea level. This training procedure is standard for all USAF aircrew recruits. DCS rarely occurs with this protocol (Rice, Vacchiano, Moore Jr., & Anderson, 2003) and no subjects in this study experienced DCS symptoms.

2.3 | Imaging protocols

All imaging data were collected at the Wilford Hall Ambulatory Surgical Center, 59th Medical Wing, Joint Base San Antonio-Lackland, TX, using a Siemens 3T Verio scanner equipped with a 32-channel phase array coil operated under quality control and assurance guidelines in accordance with recommendations by the American College of Radiology. The imaging protocol was composed of two structural (FLAIR and DTI) and two physiological (CBF and $^1\text{H-MRS}$) measurements. Imaging was performed at the baseline and then 24 and 72 hr following active exposure/sham in subjects/controls.

2.3.1 | Volumetric three-dimensional FLAIR

Three-dimensional FLAIR was utilized for analysis of white matter hyperintensities (WMH) as previously described (McGuire et al., 2012). Briefly, FLAIR images were co-registered to a common Talairach-atlas-based stereotactic frame. An experienced neuroanatomist blinded to the group manually traced WMH, while a neuroradiologist provided MRI interpretation. For each lobe we manually counted the number of WMH and used freely available Mango software (<http://ric.uthscsa.edu/Mango>; RRID:SCR_009603) to compute the total volume of WMH. WMH were divided into periependymal (adjacent to the ventricles) and subcortical (McGuire et al., 2013). Three-dimensional imaging parameters were T1 magnetization-prepared rapid gradient echo: repetition time (TR) = 2,200 ms, echo time (TE) = 2.85 ms, isotropic resolution 0.80 mm and FLAIR: TR = 4,500 ms, TE = 1 ms, and isotropic resolution 1.00 mm. FLAIR was not collected on MRI#2.

2.3.2 | High angular resolution diffusion imaging

High angular resolution diffusion imaging (HARDI) was utilized for DTI and fractional anisotropy (FA) as previously reported (McGuire et al., 2016). Briefly, DTI data were collected using a single-shot echo-planar, single refocusing spin-echo, T2-weighted sequence with a spatial resolution of $1.7 \times 1.7 \times 3.0$ mm with sequence parameters of TE/TR = 87/8,000 ms, field of view (FOV) = 200 mm, axial slice orientation with 50 slices and no gaps, 64 isotropically distributed diffusion-weighted directions, two diffusion weighting values ($b = 0$ and 700 s/mm²), and five $b = 0$ images. HARDI data for both groups were processed using the ENIGMA DTI (<http://enigma.ini.usc.edu/protocols/dti-protocols/>; RRID:SCR_014649) pipeline (Jahanshad et al., 2013). The ENIGMA-DTI analysis pipeline is based on the tract-based spatial statistics method, distributed as a part of FSL package (Smith et al., 2006) and consists of a set of protocols and scripts to measure average whole-brain FA value and average tract FA values for 10 major WM tracts (corpus callosum, corticospinal, internal capsule, corona radiata, thalamic radiation, sagittal stratum, external capsule, cingulum, superior longitudinal fasciculus, and fronto-occipital). The ENIGMA-DTI pipeline incorporates visual and quantitative quality assurance (QA) and control analyses. It includes visual inspection and two quantitative QA estimates: average motion and average projection distance. Prior research showed that FA estimates provided by this pipeline may become unstable if the average motion exceeds 2.5 mm and average projection distance exceeds 3.8 mm (Acheson et al., 2017).

2.3.3 | Pseudo-continuous arterial spin labeling (pCASL) imaging

Pseudo-continuous arterial spin labeling (pCASL; RRID:SCR_015004) imaging data for gray and WM were collected using gradient-echo echo-planar imaging with TE/TR = 16/4,000 ms, labeling duration = 2.1 s, 24 contiguous slices with 5-mm slice thickness, matrix = 64×64 , $3.4 \times 3.4 \times 5.0$ -mm resolution (FOV = 220 mm) labeling gradient = 0.6 G/cm, bandwidth = 1,594 Hz/pixel, 136 measurements, labeling offset = 90 mm, labeling duration = 2,100 ms, postlabeling delay = 0.93 s. In total, 68 alternating labeled and unlabeled image pairs were collected. Equilibrium

magnetization (M₀) images were collected using a long TR = 10 s protocol. pCASL data were processed using the pipeline described elsewhere (<http://www.mccauslandcenter.sc.edu/CRNL/tools/asl>). Labeled and unlabeled pCASL images were independently motion-corrected and a combined mean image was computed and co-registered to the spatially normalized T1W anatomical image. Perfusion weighted images were calculated by voxel-wise subtractions of unlabeled and labeled images resulting in a mean perfusion weighted image. Absolute WM perfusion or WM CBF (blood flow and perfusion are interchangeable terms here) quantification was calculated in native space from the mean perfusion images. Voxel-wise perfusion, in mL per 100 g per minute, was calculated under the assumption that the post-label delay was longer than average transfer time (Wang et al., 2002), where labeling efficiency was set at 0.99 and the mean transit time was set to 0.7 s based on empirical data (Wey, Wang, & Duong, 2011). While this protocol deviated from the consensus guidelines derived from aged subjects (Alsop et al., 2015), it was developed empirically to maximize detection of WM perfusion by increasing labeling efficiency and signal-to-noise ratio of the pCASL protocol (van Gelderen, de Zwart, & Duyn, 2008; Wey et al., 2011). We used a sample of five subjects from this study to ensure that the derived parameters take into account the geometry of the MRI scanner and incorporate vascular physiology aspects of the subjects in this sample.

2.3.4 | Proton magnetic resonance spectroscopy (¹H-MRS)

Proton MRS data were acquired from voxels placed in the anterior cingulate (ACC) using the point resolved spectroscopy sequence with the following parameters: TE = 30 ms, TR = 1,500 ms, NEX = 256, 1.2-kHz spectral width, 1,024 complex points, VOI = 6 cm³. A water reference (NEX = 8) was collected to be used as a reference and for phase and eddy current correction. A basis set of 19 metabolites was simulated using the GAVA (gamma visual analysis; RRID:SCR_003430) software (Soher, Young, Bernstein, Aygula, & Maudsley, 2007) package for use in quantifying the 30-ms TE ¹H-MRS data: alanine, aspartate, creatine (Cr), γ -aminobutyric acid, glucose, glutamate (Glu), glutamine (Gln), glutathione (GSH), glycine, glycerophosphocholine, lactate, myo-inositol (MI), *N*-acetylaspartate (NAA), *N*-acetylasparylglutamate, phosphocholine (Cho), phosphocreatine, phosphoroylethanolamine, scyllo-inositol, and taurine. Metabolite levels were reported in institutional units, and all metabolites with percent standard deviation Cramer-Rao lower bounds $\leq 20\%$ were included in statistical analyses. The ACC region is a mixture of gray and WM and therefore metabolite levels were corrected for the proportion of GM, WM, and CSF within the spectroscopic voxel using in-house Matlab code based directly on the work of Gasparovic (Gasparovic et al., 2006). More specifically, tissue segmentation was performed in Statistical Parametric Mapping 8 (SPM8) (Wellcome-Trust-Centre-for-Neuroimaging, 2015) using the T1W images acquired for voxel positioning to obtain the fraction of GM, WM, and CSF.

2.4 | Statistical analysis

2.4.1 | Analysis of covariance

Analysis of covariance (ANCOVA) was used to examine the omnibus effects of exposure related structural (FLAIR and DWI) and physiological

(CBF and neurochemical) changes occurring between (a) baseline and 24 hr postexposure and (b) baseline and 72 hr postexposure. The first ANCOVA included age and was performed in subjects and controls separately. A second ANCOVA included age and group (AFC vs. NOR) and evaluated group differences.

2.4.2 | Factor analysis of MRS measured neurochemicals

We used factor analysis to reduce the number of dependent variables and co-linearity among the MRS measurements. Baseline concentrations of Glutamate/Glutamine (GluGln), GSH, Cho, NAA, MI, and Cr were entered into a principle component analysis (PCA). A varimax rotation orthogonalized the individual eigenvectors and two factors (Factor1 and Factor2) were extracted for GLME analyses.

2.4.3 | Generalized linear mixed effects model

We used two separate generalized linear mixed effects (GLME) models to (a) assess the effect of hypobaric exposure on CBF and (b) assess the predictability of baseline neuroprotective and neuro-inflammatory MRS factors for CBF trajectories. All GLME modeling was performed in R (<http://www.R-project.org>) using the nonlinear mixed effect (NLME) model library (Pinheiro, Bates, DebRoy, & Sarkar, 2008). The GLME model determines fixed (predictor) effects observed on the group level and a random set of latent, nonindependent effects unique to each subject. Significance was set at $p \leq .05$.

The first GLME model included age, group, and MRI session as fixed predictors for CBF, and a random effect variable to account for individual variance. The model for WM ASL, is shown in Equation (1):

$$\text{WM ASL} = \beta_{\text{MRI} \cdot \text{Group} \cdot \text{Age}} \cdot \text{MRI} \cdot \text{Group} \cdot \text{Age} + \alpha_{i,j} \quad (1)$$

where MRI is the session number (1 or 2); group is the control or experimental group (0 or 1, respectively); age is the age of the subject

TABLE 1 CBF values (mean \pm SEM) for each MRI by group

Imaging session	AFC	NOR	ANCOVA p-value
	Mean CBF \pm SE (mL/100 g/min)	Mean CBF \pm SE (mL/100 g/min)	
<i>White matter</i>			
MRI#1	7.045 \pm 0.171	7.003 \pm 0.199	-
MRI#2	7.311 \pm 0.161	6.909 \pm 0.194	.022
MRI#3	7.255 \pm 0.162	7.083 \pm 0.193	.597
<i>Gray matter</i>			
MRI#1	50.160 \pm 0.762	50.798 \pm 1.054	-
MRI#2	50.691 \pm 0.753	50.713 \pm 1.032	.567
MRI#3	50.918 \pm 0.785	50.570 \pm 1.054	.591

ANCOVA significance of MRI#2 and MRI#3 relative to baseline MRI#1. MRI# and imaging session are used interchangeably. Abbreviations: AFC, exposed aircrew subjects; ANCOVA, analysis of covariance; CBF, cerebral blood flow; MRI, magnetic resonance imaging; NOR, matched controls; SEM, standard error.

at the imaging session; and $\alpha(i,j)$ is random effects of the "ith" subject on the "jth" imaging session. The main analysis was restricted to males only. However, supplementary analyses were performed that included female subjects and accounted for sex as a predictor.

A second GLME model included the neuroprotective and neuro-inflammatory factors as fixed predictors. This model, when written for WM ASL with the factors, is shown in Equation (2).

$$\text{WM ASL} = \beta_{\text{MRI} \cdot \text{Group} \cdot \text{Age}} \cdot \text{MRI} \cdot \text{Group} \cdot \text{Age} + \beta_{\text{Factor1} \cdot \text{MRI} \cdot \text{Group} \cdot \text{Age}} \cdot \text{Factor1} \cdot \text{MRI} \cdot \text{Group} \cdot \text{Age} + \beta_{\text{Factor2} \cdot \text{MRI} \cdot \text{Group} \cdot \text{Age}} \cdot \text{Factor2} \cdot \text{MRI} \cdot \text{Group} \cdot \text{Age} + \alpha_{i,j} \quad (2)$$

3 | RESULTS

ANCOVA demonstrated a significant elevation ($p = .022$) in WM CBF between baseline and 24-hr postexposure in aircrew (AFC) subjects (Table 1). The WM CBF remained elevated at 72-hr versus baseline but not significantly ($p = .597$). There were no significant changes in GM CBF or structural (FLAIR and FA) measurements (Table 1/Table 2).

The elevation in WM CBF was replicated using the GLME model 1 (Equation 1) with baseline and 24-hr postexposure imaging points. It demonstrated a significant Session:Group ($p = .017$) and Session:Age:Group ($p = .038$) interaction (Table 3). GM-ASL trended for Session:Group ($p = .079$) which was nonsignificant with inclusion of Age ($p = .101$).

We used factor analysis to calculate two orthogonal ^1H -MRS based predictors of individual CBF changes in response to exposure. Factor 1 captured 29.1% of the variance and loaded on MI, Cho, and Cr. Factor 2 captured 28.3% of the variance and loaded on GSH, NAA, and GluGln (Table 4).

TABLE 2 ANCOVA p-value results for structural and physiological measurements

Measurement	ANCOVA p-value MRI#1 – MRI#2	ANCOVA p-value MRI#1 – MRI#3
LNFLAIR		.236
Total lesion count		.207
Subcortical volume		.790
Periependymal volume		.113
Subcortical count		.623
Periependymal count		.155
Average FA	.663	.796
GSH	.483	.364
Cho	.833	.656
NAA	.788	.980
MI	.940	.383
Cr	.995	.551
Glu/Gln	.833	.537

ANCOVA, analysis of covariance; Cho, phosphocholine; Cr, creatine; FA, fractional anisotropy; Glu/Gln, glutamate/glutamine; GSH, glutathione; LNFLAIR, natural logarithm of fluid-attenuated inversion recovery white matter hyperintensity; MI, myo-inositol; MRI, magnetic resonance imaging; NAA, N-acetylaspartate.

The second GLME model (Equation (2)) included the two factors (Factor 1—Cho, MI, Cr; Factor 2—GSH, NAA, Glu/Gln) for WM-ASL and showed significant Session:Group and Session:Group:Age interactions ($p = .014/0.035$, respectively; Table 3) with lower baseline neurometabolites levels correlating with greater increase in CBF. Factor 1 showed a trend towards significance ($p = .095$) while Factor 2 was significant $p = .0000761$). Factor 2:Group was also significant ($p = .031$). GM-ASL trended towards significance for Session:Group, Session:Group:Age, and Factor 1 ($p = .057/0.0798/0.053$ respectively). Factor 2 and Factor 2:Group were significant ($p = .0000182/0.0102$, respectively).

4 | DISCUSSION

The symptoms and neuroimaging findings following occupational hypobaric exposure resemble the pattern of focal and diffuse axonal injury in cerebral WM as reported in TBI (Fehily & Fitzgerald, 2017; Hundemer et al., 2012; Inglese et al., 2005; Jersey et al., 2011; Koerte, Ertl-Wagner, Reiser, Zafonte, & Shenton, 2012; Tate et al., 2016). We used an MRI imaging protocol to capture cerebral structure and

TABLE 4 Factor analysis revealed two factors that captured 57.4% of the variance

Component	Factor 1 (29.1% of variance)	Factor 2 (28.3% of variance)
GSH	0.269	0.665
Cho	0.691	0.164
NAA	0.187	0.686
MI	0.738	0.351
Cr	0.670	0.501
Glu/Gln	0.408	0.615

Cho, phosphocholine; Cr, creatine; Glu/Gln, glutamate/glutamine; GSH, glutathione; MI, myo-inositol; NAA, N-acetylaspartate.

physiology at three time points: 24 hr before and 24 hr and 72 hr postexposure. There were no significant changes in structural WM integrity. We observed significant elevation in WM CBF at 24 hr post-hypobaric exposure that did not return to baseline at 72 hr post-exposure. The change in CBF was inversely proportional to the baseline levels of neurochemicals associated with neuroprotection

TABLE 3 Model 1 and 2 regression results for the fixed factors (beta and p-values) between MRI#1 and #2 in AFC and NOR males

Fixed factor	Model 1		Model 2	
	β -value \pm SEM	p-value	β -value \pm SEM	p-value
WM-ASL				
Group	-1.678 \pm 2.238	.454	0.092 \pm 2.240	.967
MRI	-0.881 \pm 0.567	.123	-0.956 \pm 0.575	.099
Age	-0.080 \pm 0.052	.132	-6.89E-05 \pm 0.054	.999
Factor1			0.209 \pm 0.124	.095
Factor2			0.612 \pm 0.149	7.61E-05
MRI:Group	2.656 \pm 1.092	.017	2.735 \pm 1.100	.014
MRI:Age	0.036 \pm 0.025	.151	0.038 \pm 0.025	.132
Group:Age	0.061 \pm 0.104	.560	-0.016 \pm 0.103	.877
Group:Factor1			-0.080 \pm 0.205	.696
Group:Factor2			-0.448 \pm 0.205	.031
MRI:Group:Age	-0.106 \pm 0.051	.038	-0.109 \pm 0.051	.035
GM-ASL				
Group	-9.682 \pm 11.470	.399	-1.365 \pm 11.193	.903
MRI	-3.845 \pm 5.982	.198	-4.427 \pm 2.940	.135
Age	-0.437 \pm 0.264	.099	-0.043 \pm 0.270	.875
Factor1			1.181 \pm 0.603	.053
Factor2			3.244 \pm 0.724	1.82E-05
MRI:Group	10.124 \pm 5.719	.079	10.827 \pm 5.620	.057
MRI:Age	0.175 \pm 0.131	.185	0.192 \pm 0.129	.141
Group:Age	0.379 \pm 0.532	.477	0.009 \pm 0.517	.987
Group:Factor1			-0.747 \pm 0.994	.454
Group:Factor2			-2.602 \pm 0.995	.010
MRI:Group:Age	-0.438 \pm 0.265	.101	-0.459 \pm 0.260	.080

Bolded values indicate significance ($p \leq .05$).

Abbreviations: AFC, exposed aircrew subjects; ASL, arterial spin labeling; GM, gray matter; MRI, magnetic resonance imaging; NOR, matched controls; WM, white matter.

TABLE 5 Model 1 regression results for the fixed factors (beta and p-values) between MRI#1 and #2 in AFC males and females

Fixed factor	Model 1	
	β -value \pm SEM	p-value
WM-ASL		
Sex	5.507 \pm 3.182	.085
MRI	1.740 \pm 1.122	.124
Age	-0.019 \pm 0.097	.846
MRI:Sex	-0.613 \pm 1.732	.724
MRI:Age	-0.069 \pm 0.053	.198
Sex:Age	0.208 \pm 0.148	.161
MRI:Sex:Age	0.035 \pm 0.081	.663
GM-ASL		
Sex	22.961 \pm 0.470	.139
MRI	6.186 \pm 5.282	.245
Age	-0.062 \pm 0.470	.895
MRI:Sex	-1.100 \pm 8.156	.893
MRI:Age	-0.260 \pm 0.249	.299
Sex:Age	-0.848 \pm 0.532	.239
MRI:Sex:Age	0.082 \pm 0.265	.829

AFC, exposed aircrew subjects; ASL, arterial spin labeling; GM, gray matter; MRI, magnetic resonance imaging; WM, white matter.

and maintenance of normal WM physiology. We conclude that hypobaric exposure in aircrew undergoing basic training leads to up-regulated WM CBF without observable structural changes and therefore constitutes a valuable model for studying WM repair mechanisms. This finding is an important consideration with respect to the aircraft-based evacuation of patients with TBI where elevation in WM CBF may worsen the clinical outcomes.

The mechanisms of hypobaric damage to cerebral WM are unknown. Both hypo- and hyperbaric exposure in aviators and divers has been associated with venous and arterial microbubbles (Balladin, Pilmanis, & Webb, 2004; Pilmanis, Meissner, & Olson, 1996; Vann, Butler, Mitchell, & Moon, 2011) and in divers, the production of blood-borne micro particles (Thom et al., 2012). The transient tissue hypoxia following the occlusion of micro-capillaries may trigger an innate immune response leading to diffuse axonal injury. Cerebral WM in the frontal and parietal areas is particularly vulnerable to hypo- and hyperbaric brain injury (McGuire et al., 2013). These regions are perfused by long, low-caliber vessels, have a large density of micro-capillaries that lack supplemental circulation, and are susceptible to transient hypoxia due to the presence of microemboli in the blood. Any activation of innate immune responses to the transient hypoxia may lead to a diffuse axonal injury that is detectable on MRI or may be assessed clinically through reduced neurocognitive scores.

The WM CBF response occurred in the absence of detectable structural differences, but the baseline concentration of CNS metabolites associated with brain protection predicted the degree of up-regulation in WM CBF. $^1\text{H-MRS}$ measurements were used to provide baseline levels of the metabolites representative of neuronal integrity/function (NAA), cellular

energy stores (Cr), membrane integrity (Cho), neuroplasticity (GluGln), glial marker suggestive of inflammation (MI), and oxidative stress (GSH; Erecinska & Silver, 1990; Kirov et al., 2013; Koerte et al., 2015). Subjects with lower baseline levels of the neurometabolites showed progressively higher CBF response in cerebral WM. This complements $^1\text{H-MRS}$ findings regarding mild TBI that report reduced NAA, suggesting axonal dysfunction rather than severe axonal injury (Kirov et al., 2013). In more severe TBI cases, such as those concerning professional soccer players, elevation in Cho and MI directly correlates with the frequency of impact

TABLE 6 Model 1 regression results for the fixed factors (beta and p-values) between MRI#1 and #2 in AFC and NOR males and females

Fixed factor	Model 1	
	β -value \pm SEM	p-value
WM-ASL		
Group	-1.674 \pm 2.319	.471
Age	-0.078 \pm 0.053	.145
MRI	-0.884 \pm 0.611	.150
Sex	-1.962 \pm 4.681	.675
Group:Age	0.060 \pm 0.107	.575
Group:MRI	2.649 \pm 1.176	.026
Age:MRI	0.036 \pm 0.027	.181
Group:Sex	7.495 \pm 5.595	.181
Age:Sex	0.151 \pm 0.180	.401
MRI:Sex	1.636 \pm 2.365	.490
Group:Age:MRI	-0.106 \pm 0.054	.054
Group:Age:Sex	-0.360 \pm 0.230	.117
Group:MRI:Sex	-2.274 \pm 2.828	.423
Age:MRI:Sex	-0.048 \pm 0.091	.601
Group:Age:MRI:Sex	0.084 \pm 0.116	.471
GM-ASL		
Group	-9.676 \pm 11.932	.418
Age	-0.438 \pm 0.275	.113
MRI	-3.851 \pm 3.135	.221
Sex	-9.148 \pm 24.089	.704
Group:Age	0.378 \pm 0.553	.495
Group:MRI	10.112 \pm 6.035	.096
Age:MRI	0.175 \pm 0.138	.208
Group:Sex	32.182 \pm 28.790	.264
Age:Sex	0.761 \pm 0.926	.412
MRI:Sex	6.533 \pm 12.134	.591
Group:Age:MRI	-0.437 \pm 0.279	.120
Group:Age:Sex	-1.611 \pm 1.181	.174
Group:MRI:Sex	-7.701 \pm 14.153	.596
Age:MRI:Sex	-0.226 \pm 0.466	.629
Group:Age:MRI:Sex	0.311 \pm 0.595	.603

AFC, exposed aircrew subjects; ASL, arterial spin labeling; GM, gray matter; MRI, magnetic resonance imaging; NOR, matched controls; WM, white matter.

suggesting an association between neuroinflammation markers and subconcussive head trauma (Koerte et al., 2015).

There were no significant changes in structural indices of WM integrity at 24 and 72 hr postexposure. Similarly, we observed no effect on the baseline FA and WMH volume measures or on the changes in WM CBF following exposure. The consistency may be due in part to the participants' uniformly sound health, young age, and high level of physical fitness. All subjects had very minor WMH burden consistent with their age and health status (McGuire, Sherman, et al., 2014). Overall, our research supports the safety of the hypobaric exposure protocol as used by the USAF with a 0.26% clinical incidence of DCS (Rice et al., 2003).

Our findings have immediate relevance to clinical practice because injured members of US armed forces, including those on active duty who have sustained blast and other types of acute brain injury, are often evacuated by air transport. This exposes patients with brain injury to several hours of mild hypobaric exposure (8,000 ft. pressurized cabin altitude), which may elevate their WM CBF, inadvertently worsening their clinical outcomes.

This study has two potential limitations. We believe the dominant factor in this CBF change was hypobaria rather than the brief (2–4 min) hypoxia based on prior research on CBF and hypoxia (Arnglim et al., 2016; Lawley et al., 2014). Lawley et al. (2014) noted 10 hr of normobaric hypoxia (12% O₂ inspired air; O₂ saturation 81%) was associated with an increase in CBF after 2 hr of exposure but with normalization at 10 hr postexposure Lawley et al. (2014). Arnglim et al. (2016) noted an increase in CBF at 2 hr of normobaric hypoxia (O₂ sat 70–75%) but did not report CBF 24 hr posthypoxia. We designed this study to collect imaging points at 24 and 72 hr postexposure thus eliminating the effects of a brief and minor hypoxia.

The second limitation of this study is our analyses were performed only in males due to insufficient number of female controls. However, the rates of DCS are reportedly equal for both sexes (Webb, Kannan, & Pilmanis, 2003). Furthermore, in posthoc analysis, we observed no significant difference between AFC male–female CBF changes (M/F 64/32 WM-CBF/GM-CBF $p = 0.664/0.893$ respectively). Also, no difference in response was detected when applying Model 1 to AFC males:females (Table 5; WM-ASL/GM-ASL Session:Gender:Age $p = 0.663/0.829$, respectively). Analyses in AFC:NOR males + females (AFC M/F 64/32; NOR M/F 60/5) showed no significant difference in Group:Age:Session:Gender (Table 6; WM-ASL/GM-ASL $p = .471/0.603$, respectively) reflecting the small number of control females. Future research should include sufficient female controls to facilitate analysis.

ACKNOWLEDGMENTS

The authors wish to thank Ms. Elaine "Sandy" Kawano, U.S. Air Force School of Aerospace Medicine, 711th Human Performance Wing, Wright-Patterson AFB, OH and Mrs. Trina Lion. Sheppard Pratt Hospital, Towson, MD for scientific editorial assistance, and Dr. Jisuk Park, 59th Medical Wing, Joint Base San Antonio-Lackland, TX, for statistical assistance.

Grant support was received from U.S. Air Force Surgeon General (I-11-10 and I-11-44, SAM), NIH R01MH094520 and R01MH096263 (LMR), and NIH U01MH108148, R01EB015611, and T32MH067533 (PVK).

CONFLICT OF INTERESTS

Dr. McGuire reports no disclosures. Ms. Ryan reports no disclosures. Dr. Sherman reports no disclosures. Dr. Sladky reports no disclosures. Dr. Rowland serves on the editorial board of Schizophrenia Bulletin. Dr. Wijtenburg reports no disclosures. Dr. Hong reports no disclosures. Dr. Kochunov serves on the editorial board of Human Brain Mapping and NeuroImage. The views expressed in this article are those of the authors and do not necessarily reflect the official policy or position of the Air Force, the Department of Defense, or the U.S. Government.

ORCID

Stephen A. McGuire  <https://orcid.org/0000-0001-8788-079X>

REFERENCES

- Acheson, A., Wijtenburg, S. A., Rowland, L. M., Winkler, A., Mathias, C. W., Hong, L. E., ... Dougherty, D. M. (2017). Reproducibility of tract-based white matter microstructural measures using the ENIGMA-DTI protocol. *Brain and Behavior: A Cognitive Neuroscience Perspective*, 7(2), e00615.
- Adams, J. H., Graham, D. I., Murray, L. S., & Scott, G. (1982). Diffuse axonal injury due to nonmissile head injury in humans: An analysis of 45 cases. *Annals of Neurology*, 12(6), 557–563.
- Alsop, D. C., Detre, J. A., Golay, X., Gunther, M., Hendrikse, J., Hernandez-Garcia, L., ... Zaharchuk, G. (2015). Recommended implementation of arterial spin-labeled perfusion MRI for clinical applications: A consensus of the ISMRM perfusion study group and the European consortium for ASL in dementia. *Magnetic Resonance in Medicine*, 73(1), 102–116.
- Arnglim, N., Schytz, H. W., Britze, J., Amin, F. M., Vestergaard, M. B., Hougaard, A., ... Ashina, M. (2016). Migraine induced by hypoxia: An MRI spectroscopy and angiography study. *Brain*, 139(Pt 3), 723–737.
- Ballin, U. I., Pilmanis, A. A., & Webb, J. T. (2004). Central nervous system decompression sickness and venous gas emboli in hypobaric conditions. *Aviation, Space, and Environmental Medicine*, 75(11), 969–972.
- Connolly, D. M., & Lee, V. M. (2015). Odds ratio meta-analysis and increased prevalence of white matter injury in healthy divers. *Aerospace Medicine and Human Performance*, 86(11), 928–935.
- DoD. 2011DoD Instruction 3216.02, 3216.02 Protection of human subjects and adherence to ethical standards in DoD-supported research. Department of Defense.
- Erecinska, M., & Silver, I. A. (1990). Metabolism and role of glutamate in mammalian brain. *Progress in Neurobiology*, 35(4), 245–296.
- Fayed, N., Modrego, P. J., & Morales, H. (2006). Evidence of brain damage after high-altitude climbing by means of magnetic resonance imaging. *The American Journal of Medicine*, 119(2), 168 e161–168 e166.
- Fehily, B., & Fitzgerald, M. (2017). Repeated mild traumatic brain injury: Potential mechanisms of damage. *Cell Transplantation*, 26(7), 1131–1155.
- Gasparovic, C., Song, T., Devier, D., Bockholt, H. J., Caprihan, A., Mullins, P. G., ... Morrison, L. A. (2006). Use of tissue water as a concentration reference for proton spectroscopic imaging. *Magnetic Resonance in Medicine*, 55(6), 1219–1226.
- Gentry, J., Rango, J., Zhang, J., & Biedermann, S. (2017). Latent presentation of decompression sickness after altitude chamber training in an active duty flier. *Aerospace Medicine and Human Performance*, 88(4), 427–430.

- Hackett, P. H., Yarnell, P. R., Hill, R., Reynard, K., Heit, J., & McCormick, J. (1998). High-altitude cerebral edema evaluated with magnetic resonance imaging: Clinical correlation and pathophysiology. *JAMA*, *280*(22), 1920–1925.
- Holleran, L., Kim, J. H., Gangolli, M., Stein, T., Alvarez, V., McKee, A., & Brody, D. L. (2017). Axonal disruption in white matter underlying cortical sulcus tau pathology in chronic traumatic encephalopathy. *Acta Neuropathologica*, *133*(3), 367–380.
- Hundemer, G. L., Jersey, S. L., Stuart, R. P., Butler, W. P., & Pilmanis, A. A. (2012). Altitude decompression sickness incidence among U-2 pilots: 1994–2010. *Aviation, Space, and Environmental Medicine*, *83*(10), 968–974.
- Inglese, M., Makani, S., Johnson, G., Cohen, B. A., Silver, J. A., Gonen, O., & Grossman, R. I. (2005). Diffuse axonal injury in mild traumatic brain injury: A diffusion tensor imaging study. *Journal of Neurosurgery*, *103*(2), 298–303.
- Jahanshad, N., Kochunov, P., Sprooten, E., Mandl, R. C., Nichols, T. E., Almasy, L., ... Glahn, D. C. (2013). Multi-site genetic analysis of diffusion images and voxelwise heritability analysis: A pilot project of the ENIGMA-DTI working group. *NeuroImage* doi:pii: S1053-8119(13)00408-4. 10.1016/j.neuroimage.2013.04.061, *81*, 455–469.
- Jersey, S. L., Hundemer, G. L., Stuart, R. P., West, K. N., Michaelson, R. S., & Pilmanis, A. A. (2011). Neurological altitude decompression sickness among U-2 pilots: 2002–2009. *Aviation, Space, and Environmental Medicine*, *82*(7), 673–682.
- Kirov, I. I., Tal, A., Babb, J. S., Lui, Y. W., Grossman, R. I., & Gonen, O. (2013). Diffuse axonal injury in mild traumatic brain injury: A 3D multivoxel proton MR spectroscopy study. *Journal of Neurology*, *260*(1), 242–252.
- Kochunov, P., Coyle, T., Lancaster, J., Robin, D. A., Hardies, J., Kochunov, V., ... Fox, P. T. (2010). Processing speed is correlated with cerebral health markers in the frontal lobes as quantified by neuroimaging. *NeuroImage*, *49*(2), 1190–1199.
- Kochunov, P., Glahn, D., Lancaster, J., Winkler, A., Kent, J. W., Jr., Olvera, R. L., ... Blangero, J. (2010). Whole brain and regional hyperintense white matter volume and blood pressure: Overlap of genetic loci produced by bivariate, whole-genome linkage analyses. *Stroke*, *41*(10), 2137–2142.
- Kochunov, P., Glahn, D. C., Lancaster, J., Winkler, A., Karlsgodt, K., Olvera, R. L., ... Blangero, J. (2011). Blood pressure and cerebral white matter share common genetic factors in Mexican Americans. *Hypertension*, *57*(2), 330–335.
- Kochunov, P., Robin, D., Royall, D., Lancaster, J., Kochunov, V., Coyle, T., ... Fox, P. (2009). Can structural MRI cerebral health markers track cognitive trends in executive control function during normal maturation and adulthood? *Human Brain Mapping*, *30*(8), 2581–2594.
- Koerte, I. K., Ertl-Wagner, B., Reiser, M., Zafonte, R., & Shenton, M. E. (2012). White matter integrity in the brains of professional soccer players without a symptomatic concussion. *JAMA*, *308*(18), 1859–1861.
- Koerte, I. K., Lin, A. P., Muehlmann, M., Merugumala, S., Liao, H., Starr, T., ... Shenton, M. E. (2015). Altered neurochemistry in former professional soccer players without a history of concussion. *Journal of Neurotrauma*, *32*(17), 1287–1293.
- Lawley, J. S., Alperin, N., Bagci, A. M., Lee, S. H., Mullins, P. G., Oliver, S. J., & Macdonald, J. H. (2014). Normobaric hypoxia and symptoms of acute mountain sickness: Elevated brain volume and intracranial hypertension. *Annals of Neurology*, *75*(6), 890–898.
- McGuire, S., Sherman, P., Profenna, L., Grogan, P., Sladky, J., Brown, A., ... Kochunov, P. (2013). White matter hyperintensities on MRI in high-altitude U-2 pilots. *Neurology*, *81*(8), 729–735.
- McGuire, S. A., Boone, G. R., Sherman, P. M., Tate, D. F., Wood, J. D., Patel, B., ... Kochunov, P. V. (2016). White matter integrity in high-altitude pilots exposed to Hypobaric. *Aerospace Medicine and Human Performance*, *87*(12), 983–988.
- McGuire, S. A., Sherman, P. M., Brown, A. C., Robinson, A. Y., Tate, D. F., Fox, P. T., & Kochunov, P. V. (2012). Hyperintense white matter lesions in 50 high-altitude pilots with neurologic decompression sickness. *Aviation, Space, and Environmental Medicine*, *83*(12), 1117–1122.
- McGuire, S. A., Sherman, P. M., Wijtenburg, S. A., Rowland, L. M., Grogan, P. M., Sladky, J. H., ... Kochunov, P. V. (2014). White matter hyperintensities and hypobaric exposure. *Annals of Neurology*, *76*(5), 719–726.
- McGuire, S. A., Tate, D. F., Wood, J., Sladky, J. H., McDonald, K., Sherman, P. M., ... Kochunov, P. V. (2014). Lower neurocognitive function in U-2 pilots: Relationship to white matter hyperintensities. *Neurology*, *83*(7), 638–645.
- McGuire, S. A., Wijtenburg, S. A., Sherman, P. M., Rowland, L. M., Ryan, M., Sladky, J. H., & Kochunov, P. V. (2017). Reproducibility of quantitative structural and physiological MRI measurements. *Brain and Behavior: A Cognitive Neuroscience Perspective*, *7*(9), e00759.
- Medana, I. M., & Esiri, M. M. (2003). Axonal damage: A key predictor of outcome in human CNS diseases. *Brain*, *126*(Pt 3), 515–530.
- Moen, K. G., Brezova, V., Skandsen, T., Haberg, A. K., Folvik, M., & Vik, A. (2014). Traumatic axonal injury: The prognostic value of lesion load in corpus callosum, brain stem, and thalamus in different magnetic resonance imaging sequences. *Journal of Neurotrauma*, *31*(17), 1486–1496.
- Pilmanis, A. A., Meissner, F. W., & Olson, R. M. (1996). Left ventricular gas emboli in six cases of altitude-induced decompression sickness. *Aviation, Space, and Environmental Medicine*, *67*(11), 1092–1096.
- Pinheiro, J., D. Bates, S. DebRoy and D. Sarkar. (2008). *nlme: linear and nonlinear mixed effects models*.
- Rice, G. M., Vacchiano, C. A., Moore, J. L., Jr., & Anderson, D. W. (2003). Incidence of decompression sickness in hypoxia training with and without 30-min O₂ prebreathe. *Aviation, Space, and Environmental Medicine*, *74*(1), 56–61.
- Skandsen, T., Kvistad, K. A., Solheim, O., Strand, I. H., Folvik, M., & Vik, A. (2010). Prevalence and impact of diffuse axonal injury in patients with moderate and severe head injury: A cohort study of early magnetic resonance imaging findings and 1-year outcome. *Journal of Neurosurgery*, *113*(3), 556–563.
- Smith, S. M., Jenkinson, M., Johansen-Berg, H., Rueckert, D., Nichols, T. E., Mackay, C. E., ... Behrens, T. E. (2006). Tract-based spatial statistics: Voxelwise analysis of multi-subject diffusion data. *NeuroImage*, *31*(4), 1487–1505.
- Soher, B. J., Young, K., Bernstein, A., Aygula, Z., & Maudsley, A. A. (2007). GAVA: Spectral simulation for in vivo MRS applications. *Journal of Magnetic Resonance*, *185*(2), 291–299.
- Tate, D. F., Gusman, M., Kini, J., Reid, M., Velez, C. S., Drennon, A. M., ... York, G. E. (2017). Susceptibility weighted imaging and white matter abnormality findings in service members with persistent cognitive symptoms following mild traumatic brain injury. *Military Medicine*, *182*(3), e1651–e1658.
- Tate, D. F., Wade, B. S., Velez, C. S., Drennon, A. M., Bolzenius, J., Gutman, B. A., ... York, G. E. (2016). Volumetric and shape analyses of subcortical structures in United States service members with mild traumatic brain injury. *Journal of Neurology*, *263*(10), 2065–2079.
- Thom, S. R., Milovanova, T. N., Bogush, M., Bhopale, V. M., Yang, M., Bushmann, K., ... Dujic, Z. (2012). Microparticle production, neutrophil activation, and intravascular bubbles following open-water SCUBA diving. *Journal of Applied Physiology (Bethesda, MD: 1985)*, *112*(8), 1268–1278.
- van Gelderen, P., de Zwart, J. A., & Duyn, J. H. (2008). Pitfalls of MRI measurement of white matter perfusion based on arterial spin labeling. *Magnetic Resonance in Medicine*, *59*(4), 788–795.
- Vann, R. D., Butler, F. K., Mitchell, S. J., & Moon, R. E. (2011). Decompression illness. *Lancet*, *377*(9760), 153–164.
- Wang, J., Alsop, D. C., Li, L., Listerud, J., Gonzalez-At, J. B., Schnall, M. D., & Detre, J. A. (2002). Comparison of quantitative perfusion imaging using arterial spin labeling at 1.5 and 4.0 tesla. *Magnetic Resonance in Medicine*, *48*(2), 242–254.

- Webb, J. T., Kannan, N., & Pilmanis, A. A. (2003). Gender not a factor for altitude decompression sickness risk. *Aviation, Space, and Environmental Medicine*, 74(1), 2-10.
- Wellcome-Trust-Centre-for-Neuroimaging. (2015). *Statistical parametric mapping 8 (SPM8)*. Retrieved from <http://www.fil.ion.ucl.ac.uk/spm/>.
- Wey, H. Y., Wang, D. J., & Duong, T. Q. (2011). Baseline CBF, and BOLD, CBF, and CMRO2 fMRI of visual and vibrotactile stimulations in baboons. *Journal of Cerebral Blood Flow and Metabolism*, 31(2), 715-724.
- Zhang, H., Lin, J., Sun, Y., Huang, Y., Ye, H., Wang, X., ... Zhang, J. (2012). Compromised white matter microstructural integrity after mountain

climbing: Evidence from diffusion tensor imaging. *High Altitude Medicine & Biology*, 13(2), 118-125.

How to cite this article: McGuire SA, Ryan MC, Sherman PM, et al. White matter and hypoxic hypobaria in humans. *Hum Brain Mapp*. 2019;40:3165-3173. <https://doi.org/10.1002/hbm.24587>